



Analytical and Numerical Modelling of One-Dimensional Consolidation of Stabilized Peat

Leong Sing Wong^{a*}, Shamini Somanathan^a

^a College of Graduate Studies, Universiti Tenaga Nasional, IKRAM-UNITEN Road, 43000 Kajang, Selangor, Malaysia.

Received 10 November 2018; Accepted 10 February 2019

Abstract

The objective of the paper is to compare and evaluate analytical and numerical solutions of one-dimensional consolidation of stabilized peat. The type of analytical method used to solve the problem is exact method by separation of variables and utilization of Fourier series. Plaxis 2D 8.2 Professional version software was used to find numerical solution to the problem by employing the finite element method. One-dimensional consolidation problem of stabilized peat was solved numerically and validated with the one solved analytically based on laboratory experimental results. From the results, it was discovered that the consolidation characteristics of stabilized peat evaluated numerically were found to have close approximation to those evaluated analytically. There is a novel value in developing an accurate numerical prediction for the vertical consolidation of stabilized peat considering the complexity of the soil treatment method. It must be noted that peat is highly problematic because it is produced from plant decomposition with extremely high organic matter.

Keywords: One-Dimensional Consolidation; Stabilized Peat; Analytical Method; Numerical Solution.

1. Introduction

Recent advancement of mathematical modelling in geomechanics has seen the development of numerous published research works of one-dimensional consolidation of soils by analytical and numerical methods [1-13]. Despite of that, not many analytical and numerical solutions that solved one-dimensional consolidation problem of stabilized peat were found in the literature of geomechanics. This is because not much research was done on one-dimensional consolidation problem of the stabilized soil due to the difficulty at finding suitable chemical additives that can be used to stabilize highly problematic peat. In fact, the complexity of peat stabilization is fueled by the presence of highly acidic organic substance in the soil and the soil rapid consolidation settlement. Unlike the behavior of saturated clay which is dependent on the types of mineral [14], the consolidation of peat is largely dependent on the amount of organic matter which dictates the soil long term deformation under a loading application. Consolidation is a time-dependent process involving the dissipation of porous fluid pressure and the deformation of the soil skeleton [15]. Soil consolidation is mainly caused by change in effective stress, which results from increase in total stress or decrease in pore pressure [16]. The process of consolidation must be carefully studied when evaluating the compression properties of stabilized peat. Following the success of stabilizing peat with calcium chloride and polycarboxylate induced rapid setting cement in laboratory with reference to the work of Wong [17]; standard oedometer consolidation tests were performed on the stabilized soil in order to study its consolidation characteristics. The optimal mix design for the stabilized peat specimen in the oedometer consolidation tests is comprised of 300 kg m⁻³ dosage of binder by mass of wet peat at natural moisture content of 677% (The binder is composed of 90% Portland Composite Cement and 10% fly ash in composition), 4% calcium chloride by mass of the binder, and 596 kg.m⁻³ silica sand by mass of the wet peat. The test specimen was allowed to cure in water

* Corresponding author: wongls@uniten.edu.my

 <http://dx.doi.org/10.28991/cej-2019-03091254>

➤ This is an open access article under the CC-BY license (<https://creativecommons.org/licenses/by/4.0/>).

© Authors retain all copyrights.

for 7 days before testing. It is notable that oedometer consolidation apparatus is sufficient for testing the stabilized soil due to the fact that the soil was homogeneously mixed with the binding admixtures and silica sand. As such, it could be reliably used to simulate the one-dimensional deformation and drainage characteristics of the stabilized soil as the soil dissipation of excess pore water pressure became less significant over time due to the cementation process in the stabilized soil. Furthermore, the equipment set up for oedometer testing is simple and not time consuming as compared to that of a more advanced equipment such as Rowe consolidometer. The complexity of Rowe consolidometer setup is evident in the published work of Baral et al. [18] which is about the study of radial consolidation characteristics of soft clay based on large specimens. To develop a proper understanding and to ensure the reliability of the test results, it would be helpful to back analyze and validate the experimental results based on the analytical equation with the ones developed from numerical solution using Plaxis 2D 8.2 Professional version software. As such, the paper is concentrated at evaluating the results of one-dimensional consolidation tests from standard oedometer consolidation apparatus, which were determined based on the idealization of analytical model and later, validating the results using the finite element software.

2. Terzaghi's One-Dimensional Consolidation Theory

Since the inception of classical soil mechanics, Terzaghi's one-dimensional (1D) consolidation theory for saturated soils has formed an extremely useful conceptual framework in geotechnical engineering [19]. According to Terzaghi's one-dimensional consolidation theory [20-22], the process of primary consolidation of a fully saturated soil is due to the dissipation of excess pore water pressure from the soil as a result of gradual transition of applied load from water to the soil particles. Terzaghi's theory assumed that the stress-strain relationship of soil was linear in order to simplify the solution for practical use [23]. As a common issue in geotechnical engineering, consolidation is a process that reduces the soil volume due to the dissipation of excess pore water pressures [24]. Soil is a kind of porous media and saturated soil includes pore water and soil particles [34]. According to Bardet [25], the notable assumptions of the theory are listed in the following points.

- The layer of soil is homogeneous and is laterally confined.
- The soil particles and water are incompressible.
- The flow of water is one-dimensional.
- Darcy's law describes the flow of water through the soil.
- The coefficient of permeability of the soil remains constant.
- The relationship between void ratio of the soil and effective stress is linear during a stress increment.
- The soil's own weight has negligible effects.

Therefore, the rates of volume change and excess pore water diffusion of the soil is directly related to the soil permeability. Due to the positive influence of cement hydration process at stabilizing the peat, it is expected that the stabilized soil has low permeability, thereby implying its low compressibility as a result of slow rate of volume change under a load application.

3. Idealization of One-Dimensional Consolidation of Stabilized Peat

Typical one-dimensional consolidation of a stabilized peat element under the application of a stress σ is illustrated in Figure 1. The stabilized soil element has a thickness of H and is loaded in such a way that water is only allowed to drain into top and bottom rigid porous layers. In other words, only two-way vertical drainage of water is allowed in the stabilized soil element and the width of the element is infinite so that consolidation of the element is assumed to be one-dimensional only in the vertical direction (y direction). Bardet [25] idealized Terzaghi's one-dimensional consolidation theory of soil on the basis of the formulation of Equations 1 to 11. Since flow of water in the element is one-dimensionally vertical in y direction with reference to Figure 1, it is assumed that there is no flow velocity from the element in the x and z directions and therefore, $v_x = v_z = 0$. Since Darcy's law is valid, flow velocity in the vertical y direction is given by Equation 1.

$$v_y = -k_v \frac{\partial h}{\partial y} \quad (1)$$

Where k_v = coefficient of vertical permeability, h = total head of water.

The rate of water volume change of the element in Figure 1, dV_w/dt is equal to the difference between the rates of out flow and inflow of water of the element, which were $v_y dx \times 1$ and $\left[v_y + \left(\frac{\partial v_y}{\partial y} \right) dy \right] dx \times 1$ respectively. Hence, dV_w/dt can be expressed as in Equation 2.

$$\frac{dV_w}{dt} = \left(v_y + \frac{\partial v_y}{\partial y} dy \right) dx - v_y dx = \frac{\partial v_y}{\partial y} dy dx = -k_v \frac{\partial^2 h}{\partial y^2} dx dy \quad (2)$$

Total pore water pressure is defined as the total of static pore water pressure and excess pore water pressure. Since static pore water pressure varies linearly with y , the second order derivative of static pore water pressure with respect to y is equal to zero. Thus, Equation 3 can be formulated based on Equation 2.

$$\frac{dV_w}{dt} = -\frac{k_v}{\gamma_w} \frac{\partial^2 u}{\partial y^2} dx dy \quad (3)$$

Where u is the excess pore water pressure. Since the stabilized soil is elastic, change in its void ratio de is due the change in its effective stress $d\sigma'$ and therefore, Equation 4 shows the relationship.

$$\frac{de}{1 + e_0} = m_v d\sigma' \quad (4)$$

Where e_0 is the initial void ratio and m_v is the coefficient of volume compressibility. Relationship between the change in void ratio with initial volume V_0 , solid volume V_s and void volume V_v is given in Equation 5.

$$\frac{de}{1 + e_0} = \frac{d(V_v + V_s)}{V_0} = \frac{dV_v}{V_0} = \frac{dV_v}{dx \times dy \times 1} \quad (5)$$

Where it is assumed that soil particles are incompressible ($dV_s = 0$). The change in the void volume dV_v over change in time t is given by Equation 6.

$$\frac{dV_v}{dt} = m_v \frac{\partial \sigma'}{\partial t} dx dy \quad (6)$$

With total stress σ is constant $\partial \sigma / \partial t = (\partial \sigma' / \partial t) + (\partial u / \partial t) = 0$; the differential of effective stress with respect to differential of time can be stated as in Equation 7.

$$\frac{\partial \sigma'}{\partial t} = -\frac{\partial u}{\partial t} \quad (7)$$

Since the static pore water pressure is independent of time, Equation 8 is formulated based on Equations 6 and 7.

$$\frac{dV_v}{dt} = -m_v \frac{\partial u}{\partial t} dx dy \quad (8)$$

With full saturation of the stabilized soil element, the changes in the volume of voids and water are at the same rate. This gives Equation 9.

$$\frac{dV_v}{dt} = \frac{dV_w}{dt} \quad (9)$$

Substituting Equations 8 and 9 into Equation 3, the partial differential equation is denoted as Equation 10.

$$\frac{\partial u}{\partial t} = c_v \frac{\partial^2 u}{\partial y^2} \quad (10)$$

Where c_v is referred to as the coefficient of vertical consolidation and is derived from Equation 11.

$$c_v = \frac{k_v}{\gamma_w m_v} \quad (11)$$

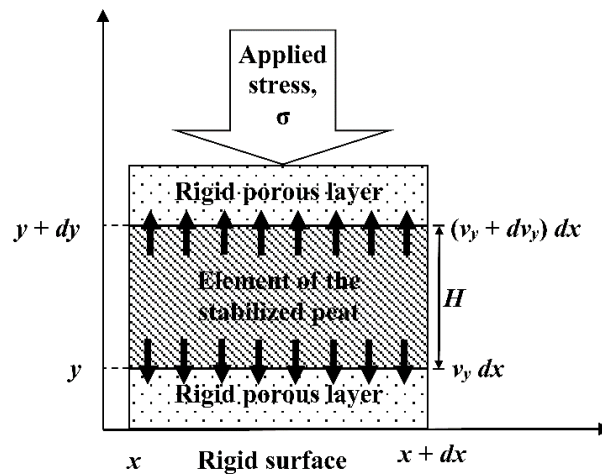


Figure 1. Element of the stabilized peat undergoing one-dimensional consolidation with two way vertical drainage (Modified from Bardet [25])

4. Analytical Method

The method employed to solve the analytical problem is by separation of variables and utilization of Fourier series. In analytical modelling, mathematical equations are proposed based on experimental data to express compression as a function of stress [26]. The analytical layer-element method is used to build relationships between displacements, stresses, and excess pore pressure and seepage velocity in the transformed domain [27]. According to Kreyszig [28], procedure to obtain the analytical solution of the method can be summarized into three steps namely, separating the variables to obtain two ordinary differential equations, determining solutions of the two ordinary differential equations that satisfy the boundary conditions, and composing the solutions using Fourier series in order to get a solution of the one-dimensional consolidation equation that satisfies the initial condition. Equation 10 is a partial differential equation with two independent variables, namely time t and vertical position y and a dependent variable, which is the excess pore water pressure, denoted as $u(y,t)$. To ensure that the c_v is positive, c_v is equated to c^2 in the formulation of the analytical solution. Thus, c_v in Equation 10 is replaced by c^2 to give Equation 12.

$$\frac{\partial u}{\partial t} = c^2 \frac{\partial^2 u}{\partial y^2} \tag{12}$$

With the one-dimensional two-way vertical drainage of water from the fully saturated stabilized peat element in Figure 1, two boundary conditions as shown in Equations 13 and 14 must be satisfied.

$$u(0, t) = 0 \text{ for } t \geq 0 \tag{13}$$

$$u(H, t) = 0 \text{ for } t \geq 0 \tag{14}$$

Since the initial excess pore water pressure at time $t = 0$ is uniform, it can be expressed as a function of $f(y)$ and the initial condition can be written as in Equation 15.

$$u(y, 0) = f(y) = u_i \text{ for } 0 < y < H \tag{15}$$

Step 1: Formulation of two ordinary differential equations.

Solution to Equation 12 is initially expressed as the product of two functions with each function is dependent on one of the variables y and t . The expression is given in Equation 16.

$$u(y,t) = F(y) G(t) \tag{16}$$

Substitution of Equation 16 into Equation 12 yields $F\dot{G} = c^2 F''G$ with $\dot{G} = dG/dt$ and $F'' = d^2F/dy^2$. Dividing the equation by c^2FG , separation of the variables is achieved and this results in Equation 17.

$$\frac{\dot{G}}{c^2G} = \frac{F''}{F} \tag{17}$$

In Equation 17, since the left expression depends only on t and the right on y , a change of t or y would only affect one side of the expressions, leaving the other side unchanged. Because of this, both sides must be constant, which is represented by k . For $k \geq 0$, the only solution for $u = FG$ that satisfies the boundary conditions is $u = 0$. Thus, for $k = -p^2$, Equation 18 is formed.

$$\frac{\dot{G}}{c^2 G} = \frac{F''}{F} = -p^2 \tag{18}$$

Equation 18 yields two linear ordinary differential equations, namely Equations 19 and 20.

$$F'' + p^2 F = 0 \tag{19}$$

$$\dot{G} + c^2 p^2 G = 0 \tag{20}$$

Step 2: Satisfying the boundary condition.

A general solution for Equation 19 is given by Equation 21.

$$F(y) = A \cos py + B \sin py \tag{21}$$

Based on the boundary conditions of Equations 13 and 14, it follows that $u(0,t) = F(0) G(t) = 0$ and $u(H,t) = F(H) G(t) = 0$. Since $G = 0$ would give $u = 0$, it is required that $F(0) = 0$ and $F(H) = 0$ in order to get $F(0) = A = 0$ by Equation 21 and then $F(H) = B \sin pH = 0$, with $B \neq 0$ (to avoid $F = 0$). As such, $\sin pH = 0$, hence $p = (2n + 1) \pi/H$ Where $n = 1, 2, 3 \dots$

Setting $B = 1$, solution to Equation 19 that satisfies Equations 13 and 14 is given by Equation 22.

$$F_{2n+1}(y) = \sin[(2n + 1)\pi / H] \text{ Where } n = 1, 2, 3 \dots \tag{22}$$

For $p = [(2n + 1)\pi / H]$, $\dot{G} + (\lambda_{2n+1})^2 G = 0$ Where $\lambda_{2n+1} = [c(2n + 1)\pi / H]$. Thus, Equation 20 has a general solution of Equation 23.

$$G_{2n+1}(t) = B_{2n+1} e^{-(\lambda_{2n+1})^2 t} \tag{23}$$

With B_{2n+1} is constant, Equations 22 and 23 are substituted into Equation 16 to give Equation 24.

$$u(y,t) = F_{2n+1}(y)G_{2n+1}(t) = B_{2n+1} \sin \frac{(2n + 1)\pi y}{H} e^{-(\lambda_{2n+1})^2 t} \tag{24}$$

Equation 24 is the solution of the one-dimensional consolidation equation that satisfies the boundary conditions. According to Kreyszig [18], it is also referred to as the eigenfunctions of the problem, corresponding to the eigenvalues, λ_{2n+1} .

Step 3: Solution of the entire problem

To develop solutions that also satisfy the initial condition, a series of eigenfunctions are given in Equation 25 based on Equation 24.

$$u(y,t) = \sum_{n=0}^{+\infty} u_{2n+1}(y,t) = \sum_{n=0}^{+\infty} B_{2n+1} \sin \frac{(2n + 1)\pi y}{H} e^{-(\lambda_{2n+1})^2 t} \tag{25}$$

Substituting Equation 15 into Equation 25, Equation 26 is obtained.

$$u(y,0) = \sum_{n=0}^{+\infty} B_{2n+1} \sin \frac{(2n + 1)\pi y}{H} = f(y) \tag{26}$$

Hence, for Equation 25 to satisfy the initial condition, B_{2n+1} 's must be the coefficients of Fourier sine series. B_{2n+1} can be written as in Equation 27.

$$B_{2n+1} = \frac{2}{H} \int_0^H f(y) \sin \frac{(2n + 1)\pi y}{H} dy, \text{ where } n = 1, 2, 3 \dots \tag{27}$$

By substituting Equation 15 into Equation 27 and solving the equation by integration, Equation 28 is yielded.

$$B_{2n+1} = \frac{2u_i}{(2n + 1)\pi} [-\cos(2n + 1)\pi + \cos 0] \tag{28}$$

For $n \geq 0$, $2n + 1$ is an odd number and as such, $\cos(2n + 1) = -1$ and since $\cos 0 = 1$, Equation 28 is solved and can be written as in Equation 29.

$$B_{2n+1} = \frac{4u_i}{(2n+1)\pi} \quad (29)$$

For two-way vertical drainage, the time t during the stabilized soil's primary consolidation in relation to c_v , H and T_v can be expressed in Equation 30.

$$t = \frac{T_v (H/2)^2}{c_v} \quad (30)$$

Where T_v = dimensionless time factor and H = drainage path. For two-way vertical drainage, the drainage path is equal to $H/2$.

Equations 29 and 30 are substituted into Equation 25 to obtain the analytical solution to the one-dimensional consolidation problem of the stabilized soil element. The analytical equation can be written as in Equation 31.

$$u(y,t) = u_i \sum_{n=0}^{+\infty} \frac{4}{(2n+1)\pi} \sin\left[\frac{(2n+1)\pi y}{H}\right] e^{-(2n+1)^2 \pi^2 T_v / 4} \quad (31)$$

Laboratory prediction on the rate of primary consolidation of the stabilized soil element can be done using curve fitting. According to Head [29], the process of comparing a laboratory consolidation curve with the theoretical one is known as curve fitting. The theoretical curve actually expresses the average degree of consolidation U as a function of theoretical time factor T_v of the stabilized soil element. Bardet [25] established Equations 32 to 38 to develop the theoretical curve. According to Bardet [25], when the change on the total stress $\Delta\sigma$ applied to the soil layer is kept constant, the change in effective stress $\Delta\sigma'(y,t)$ and excess pore water pressure $u(y,t) = 0$ in the soil layer can be related through Equation 32.

$$\Delta\sigma = u_i = \Delta\sigma'(y,t) + u(y,t) \quad (32)$$

Because primary consolidation progresses as excess pore water pressure dissipates from the stabilized soil element, it is useful to characterize the whole process in term of vertical degree of consolidation U_y as defined in Equation 33.

$$U_y = \frac{u_i - u(y,t)}{u_i} = \frac{\Delta\sigma'(y,t)}{\Delta\sigma} \quad (33)$$

Where $U_y = 0$ and $U_y = 1$ at the start and end of the soil primary consolidation respectively. It is important to note that at the start of the primary consolidation, $\Delta\sigma'(y,t) = 0$ and $u(y,t) = u_i$ and at the end of the primary consolidation, $\Delta\sigma'(y,t) = \Delta\sigma$ and $u(y,t) = 0$. For a change in the thickness of the soil element dy , the corresponding settlement is represented as ds_f after primary consolidation and as $ds(t)$ at time t during primary consolidation. These can be defined as in Equation 34.

$$ds_f = m_v \Delta\sigma dy \text{ and } ds(t) = m_v \Delta\sigma'(y,t) dy = m_v \Delta\sigma U_y dy \quad (34)$$

By integrating ds_f and $ds(t)$ in Equation 34, the corresponding total settlement and settlement at time t of the primary consolidation [s_f and $s(t)$] can be written as in Equation 35.

$$s_f = \int_0^H m_v \Delta\sigma dy = m_v H \Delta\sigma \text{ and } s(t) = \int_0^H ds(t) = \frac{s_f}{H} \int_0^H U_y dy = s_f U \quad (35)$$

Simplification of Equation 35 enables U to be defined as in Equation 36.

$$U = \frac{1}{H} \int_0^H U_y dy \quad (36)$$

Substituting Equation 31 into Equation 36 and solving by integration, U can be defined as in Equation 37.

$$U = 1 - \frac{8}{\pi^2} \sum_{n=0}^{+\infty} \frac{e^{-(2n+1)^2 \pi^2 T_v / 4}}{(2n+1)^2} \quad (37)$$

The variation of U with T_v in Equation 37 can be approximated using Equation 38 and the corresponding relationship can be plotted with U varies from 0 to 1.

$$U(T_v) = \begin{cases} U_1(T_v) = \sqrt{\frac{4}{\pi} T_v} \\ U_2(T_v) = 1 - \frac{8}{\pi^2} \exp\left(-\frac{\pi^2}{4} T_v\right) \end{cases} \quad \text{For} \quad \begin{cases} T_v < 0.2827 \\ T_v \geq 0.2827 \end{cases} \quad (38)$$

5. Numerical Method

Back analysis on the experimental results based on the solution developed from analytical method was done by validating the results with the ones generated from finite element method. This is important in order to examine the closeness of the agreement between the two solutions. The finite element method is the numerical method employed by PLAXIS 2D 8.2 Professional version software to develop numerical solution to the problem. Finite element modelling (FEM) of soil physical behavior can provide information which is difficult or impossible to obtain experimentally [30]. The basic idea in the finite element method is to find the solution of a complicated problem by replacing it by a simpler one [31]. With the simplification of the actual problem, an approximate solution rather than the exact one can be developed from the method.

It is important to note that to produce a finite element model that simulates the analytical model, the initial conditions and material properties of the model must be correctly defined. With regard to that, the finite element model was set as a plane strain model with a width of 50 mm and a height of 20 mm so as to conform to the standard size of oedometer consolidation specimen (Figure 2). A mesh consisting of 15-node triangular elements was generated for the model. The elements must be made small enough to give usable results and yet large enough to reduce computational effort [32]. The boundary conditions were set on the model in such a way that both left and right boundaries of the model were closed to water flow and consolidation (impermeable), whereas the top and bottom boundaries of the model were opened to water flow and consolidation to allow for simulation of two-way vertical drainage of excess pore water from the model. A general phreatic level was set at the same level as the top surface of the model in order to simulate full saturation at the model's initial condition. Uniformly distributed loads ranging from 50 to 800 kPa were applied incrementally on the model with a load increment ratio of 1 and the duration for each loading was 7 days. Based on laboratory experimental findings, the necessary stabilized soil parameters were inputted into the software in order to specify the material properties of the model. The stabilized soil parameters were summarized in Table 1. The type of material model used to simulate the behavior of the stabilized soil is Mohr-Coulomb model.

Numerical solution to the finite element problem is a step by step process that adheres to the procedure and formulation of numerical equations adopted by the software in accordance to Brinkgreve [33]. As a first step, the solution region was discretized into 15-node triangular finite elements after the geometry model was completely defined with boundary and load conditions, and material properties. Basically, the discretization process involved replacing the solution region having infinite elements with a mesh consisting of finite elements. According to Dhatt and Touzot [34], the finite element discretization process, like the finite difference process, transforms partial differential equations into algebraic equations. Using Galerkin procedure, the discretization process was applied to satisfy the prescribed boundary conditions. Next, an interpolation model was selected to find a suitable solution that could be used to approximate the unknown solution. The assumed solution must be simple from computational point of view, but it should satisfy certain convergence requirements [32].

Based on the assumption of the interpolation model, the element vectors (i.e. nodal displacement vector, excess pore water pressure vector, continuous displacement vector, residual force vector and incremental load vector) and matrices (i.e. strain interpolation matrix, stiffness matrix, coupling matrix and permeability matrix) were derived in equilibrium and continuity equations. Then, the element vectors and matrices were assembled and formed a block matrix equation that represented all the equilibrium and continuity equations taken into consideration. The block matrix equation was solved using a simple step by step simple integration procedure to find the unknown nodal displacements. With the nodal displacements determined, the element resultants such as stresses and strains were computed.

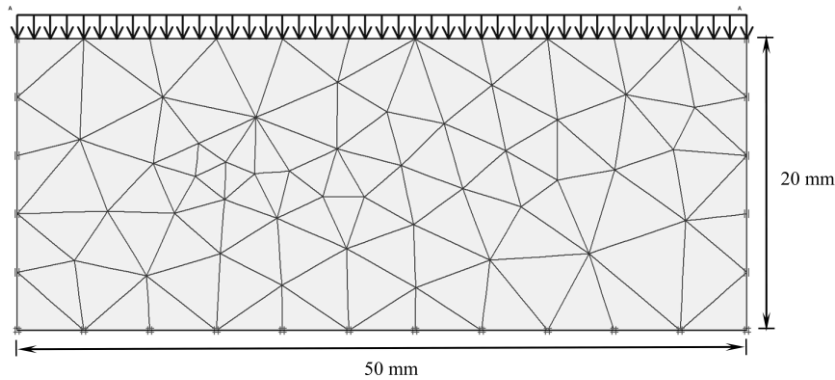


Figure 2. Finite element mesh for one-dimensional consolidation problem of the stabilized peat

Table 1. Stabilized soil parameters required for the development of the finite element model in PLAXIS 8.2 Professional version software

| Stabilized soil parameter | Parameter value |
|---|--|
| Unsaturated bulk unit weight (γ_{unsat}) | $1.240 \times 10^{-8} \text{ kN mm}^{-3}$ |
| Saturated bulk unit weight (γ_{sat}) | $1.730 \times 10^{-8} \text{ kN mm}^{-3}$ |
| Coefficient of permeability (k_v) | $3.487 \times 10^{-8} \text{ mm min}^{-1}$ |
| Young's modulus (E) | 0.010 kN mm^{-2} |
| Poisson's ratio (ν) | 0.236 |
| Cohesion (c) | $2.281 \times 10^{-4} \text{ kN mm}^{-2}$ |
| Friction angle (ϕ) | 61.190° |
| Dilatancy angle (ψ) | 0.000° |

6. Finite Element Model Validation

Square root of time method is a conventional curve fitting method that can be used to estimate c_v of the stabilized soil with reference to the time-compression data obtained from both of the laboratory experimentation and finite element software. The method determines c_v by comparing the stabilized soil compression as a function of square root of time from both experimental and numerical curves to U as a function of T_v from square root of time theoretical curve. Based on the assumption that the hydrodynamic process dominates up to 90% primary consolidation, the method determines c_v of the stabilized soil by substituting T_v as 0.848 from the square root of time theoretical curve and the time to reach 90 % of primary consolidation from experimental square root of time-compression curve into Equation 30. The values of c_v were then compared to those predicted from numerical square root of time-compression curve, which was developed from the finite element software. Based on both of the experimental and numerical time-compression curves, compression index C_c , coefficient of volume compressibility m_v , and coefficient of vertical permeability k_v estimated under the various consolidation pressures were also compared.

7. Results

Figure 3 shows the time-compression curves of the stabilized peat under the application of consolidation pressures ranging from 50 to 800 kPa, of which the data were obtained experimentally and numerically. At 20.8 days (30000 minutes) of applied loading, the numerical value for the stabilized soil compression was discovered to be 0.33 mm which overestimated the experimental compression value of the stabilized soil by 0.13 mm. However at 34.7 days (50000 minutes) of applied loading, compression of the stabilized soil measured experimentally was found to be 0.91 mm. This was slightly lower when compared to that calculated numerically at the same duration of loading with the value was observed to be 1.01 mm. Although there was a 0.10 mm difference between the two final compression values, the differential gap was very small and the shape of the numerical time-compression curve approximated closely to that of experimental time-compression curve.

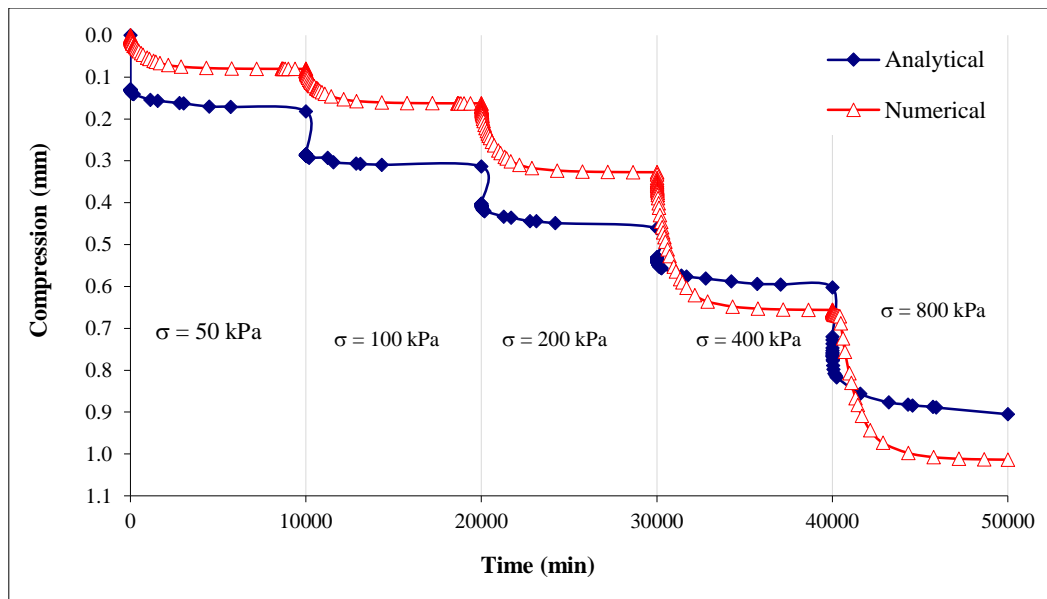


Figure 3. Time-compression behavior of the stabilized peat under various consolidation pressures

Using square root of time method and based on average degree of consolidation, graphical plots for the purpose of evaluating the rates of primary consolidation under the application of the various consolidation pressures from both experimental and finite element analyses were illustrated in Figures 4 and 5 respectively. Using the same method, the rates of primary consolidation of the stabilized soil were also determined based on the time-excess pore water pressure relationship estimated from the finite element analysis (Figure 6). From the square root of time method of interpretation of both experimental and finite element analyses, the trends of coefficients of vertical consolidation c_v with consolidation pressures of the stabilized soil were graphically depicted in Figure 7. It is evident in Figure 7 that for a range of consolidation pressures of 50 to 800 kPa, c_v was determined experimentally to vary from 0.006 to 0.013 $m^2 yr^{-1}$. Back analysis on c_v of the stabilized soil on the basis of the average degree of consolidation by finite element method revealed that the soil parameter was found to range from 0.019 to 0.024 $m^2 yr^{-1}$ under the same range of consolidation pressures. A better approximation on the range of the c_v was discovered when the coefficients were evaluated based on excess pore water pressure measurement at the center of the stabilized soil by finite element method. The c_v analyzed by the method ranged from 0.015 to 0.016 $m^2 yr^{-1}$. Over the range of consolidation pressures, it is observable from Figure 7 that both numerically predicted values of c_v for the average degree of consolidation and pore water pressure measurement of the stabilized soil tend to slightly overestimate the experimental values of c_v of the stabilized soil. Despite of the slight differences in the values of c_v of the stabilized soil evaluated experimentally and numerically, the low values of the c_v from both analyses indicated that there was a reasonable agreement between the two analyses and that the rate of compression of the stabilized soil was very low as compared to that of untreated peat, of which the c_v was found to range from 12.803 to 50.953 $m^2 yr^{-1}$ under the same range of consolidation pressures.

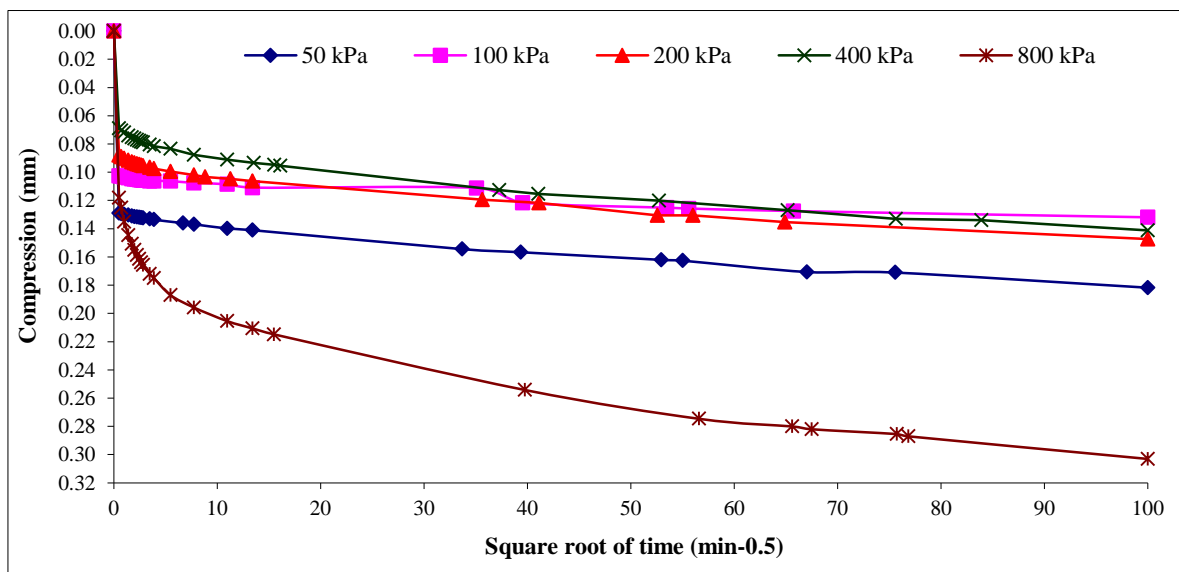


Figure 4. Square root of time-compression curves derived from experimental time-compression behavior of the stabilized peat

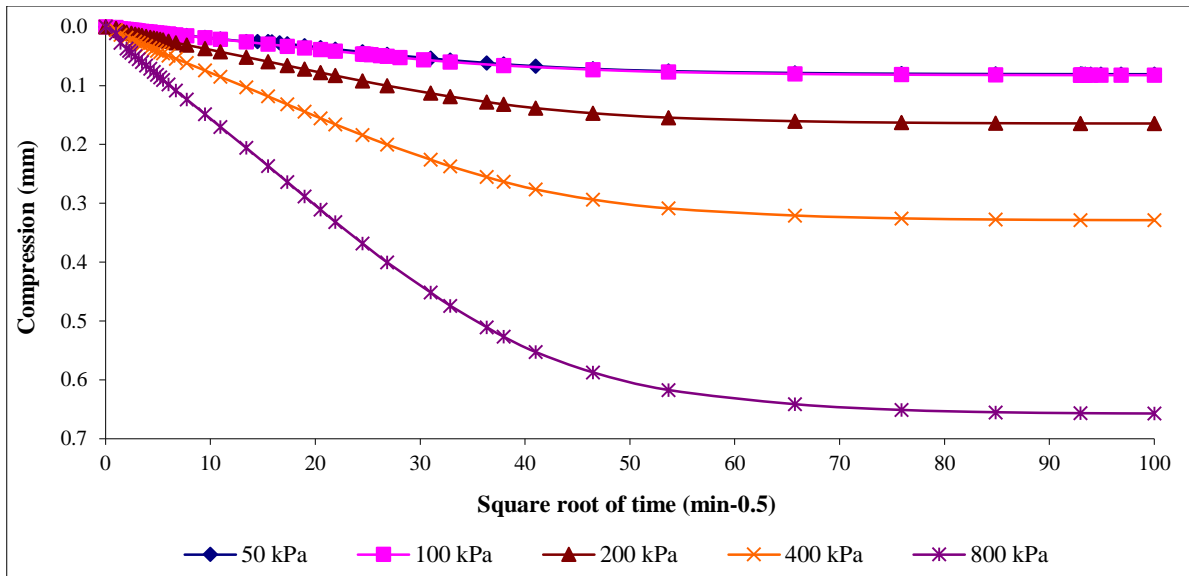


Figure 5. Square root of time-compression curves derived from numerical time-compression behavior of the stabilized peat by finite element method

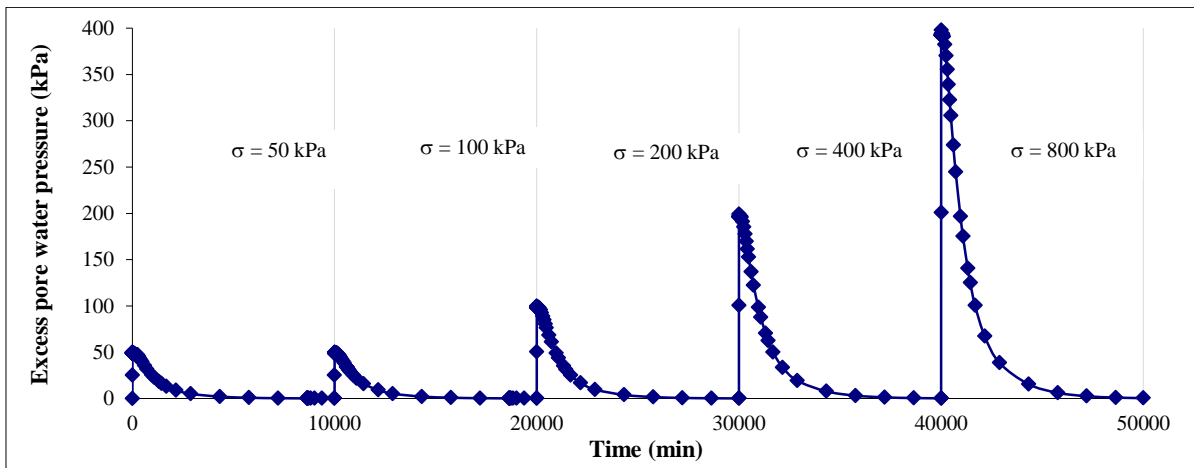


Figure 6. Time-excess pore water pressure relationship of the stabilized peat derived from numerical analysis by finite element method

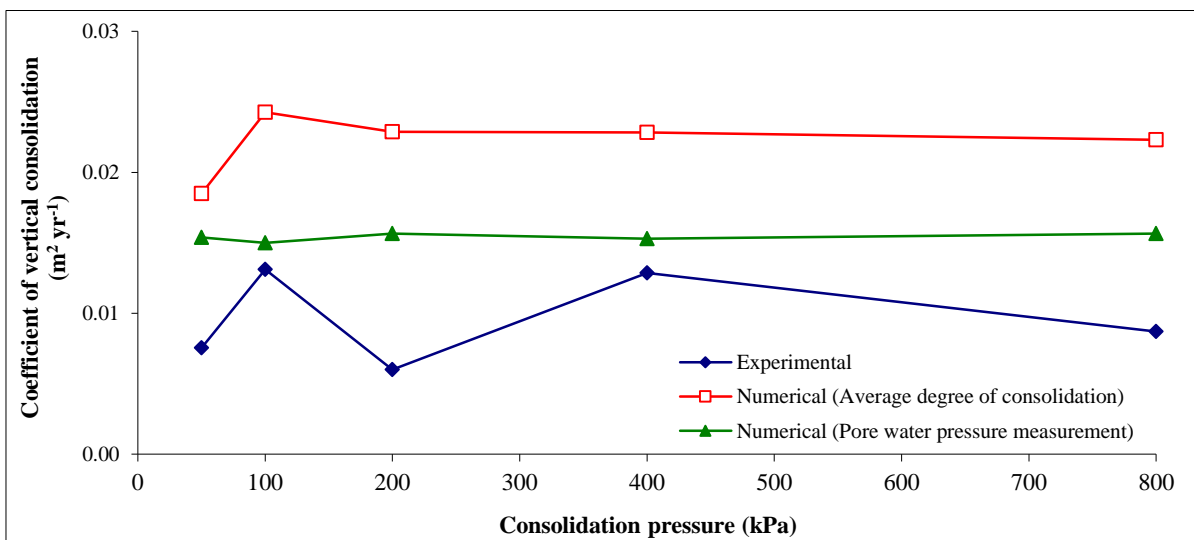


Figure 7. Trend of coefficients of vertical consolidation of the stabilized peat over a range of consolidation pressures

Based on the time-compression curves in Figure 3, the relationships between the void ratios and consolidation pressures (e -log p curves) of the stabilized soil from both experimental and numerical methods were established as shown in Figure 8. Analysis on the experimental e -log p curve in Figure 8 indicated that the C_c value of the stabilized

soil was found to be 0.113. A slightly higher value of C_c of 0.226 of the stabilized soil was determined from the numerical e -log p curve in Figure 8. Both experimental and back analyses on C_c of the stabilized soil confirmed that the stabilized soil had a very low value of C_c when compared to that of untreated peat which was found to be 3.928 by Wong et al. [35]. A good approximation of the numerical results to those obtained in the experimental tests was also found in the study of Silva et al. [28], with mean relative errors lower than 5%. Silva et al. [36] made comparison of the simulation and experimental void ratio-log vertical effective stress curves of the oedometric tests on compacted soil for water contents of 10%, 15% and 20%.

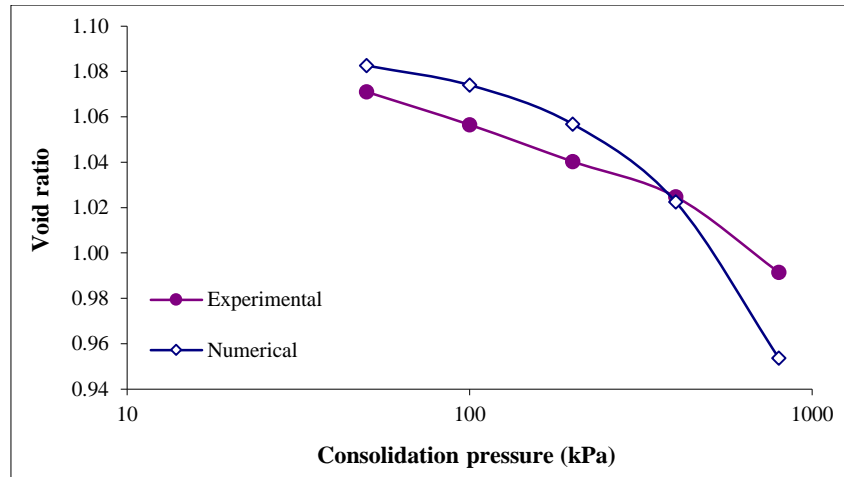


Figure 8. Void ratio-logarithm of consolidation pressure curves of the stabilized peat

With reference to the values of c_v in Figure 7 and the e -log p curves in Figure 8, m_v and k_v of the stabilized soil over the range of consolidation pressures could be determined as shown in Figures 9 and 10 respectively. It is evident in Figure 9 that experimentally, m_v of the stabilized soil was found to range from 0.037 to 0.191 $\text{m}^2 \text{MN}^{-1}$. The related numerical results of the stabilized soil in the same figure showed that the m_v ranged from 0.077 to 0.086 $\text{m}^2 \text{MN}^{-1}$. At the application of 50 kPa consolidation pressure, the numerical value of k_v for the stabilized soil was noticed to be 0.077 $\text{m}^2 \text{MN}^{-1}$ which slightly underestimated its experimental value of k_v by 0.114 $\text{m}^2 \text{MN}^{-1}$. However, when the consolidation pressure was increased to 800 kPa, the numerical value of k_v for the stabilized soil was realized to be 0.084 $\text{m}^2 \text{MN}^{-1}$ which slightly overestimated its experimental value by 0.042 $\text{m}^2 \text{MN}^{-1}$. Anyhow, both of the experimental and numerical results indicated that there was a close agreement and that m_v of the stabilized soil was very low as a result of low compressibility of the stabilized soil. The low compressibility of the stabilized soil also implied that it had low permeability under the application of various consolidation pressures as shown in Figure 10. The experimental values of k_v of the stabilized soil in Figure 10 were found to range from 1.1×10^{-13} to $5.9 \times 10^{-13} \text{ m s}^{-1}$. Their numerical values were found to range from 4.4×10^{-13} to $6.5 \times 10^{-13} \text{ m s}^{-1}$. The close approximation in the numerical values of k_v for the stabilized soil to its experimental values of k_v confirmed that it had very low permeability under the application of consolidation pressures.

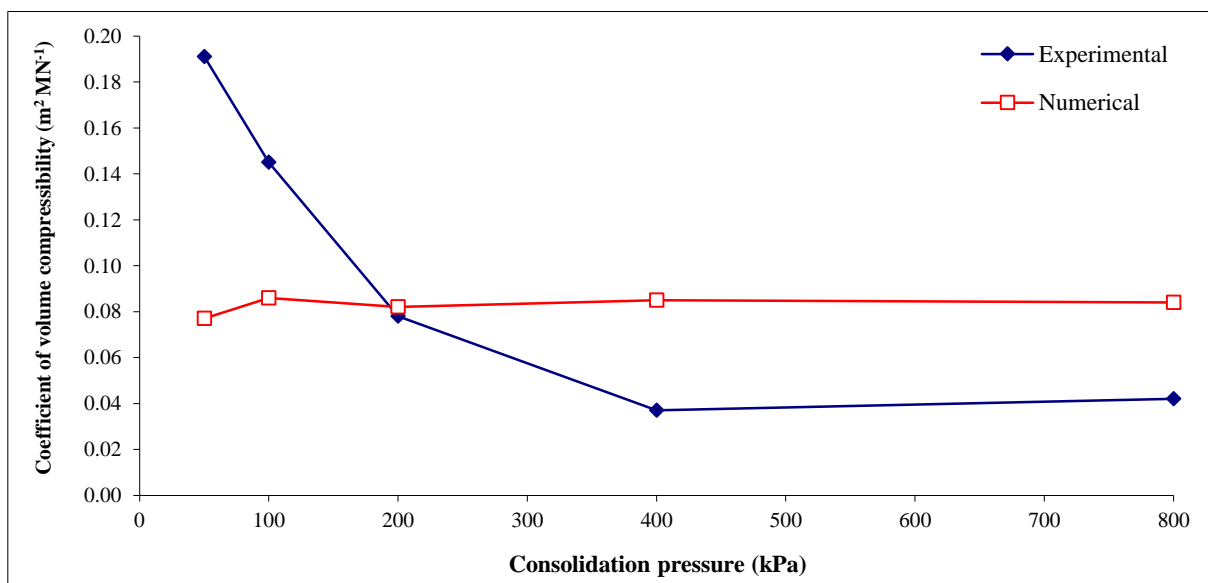


Figure 9. Trend of coefficients of volume compressibility of the stabilized peat over a range of consolidation pressures

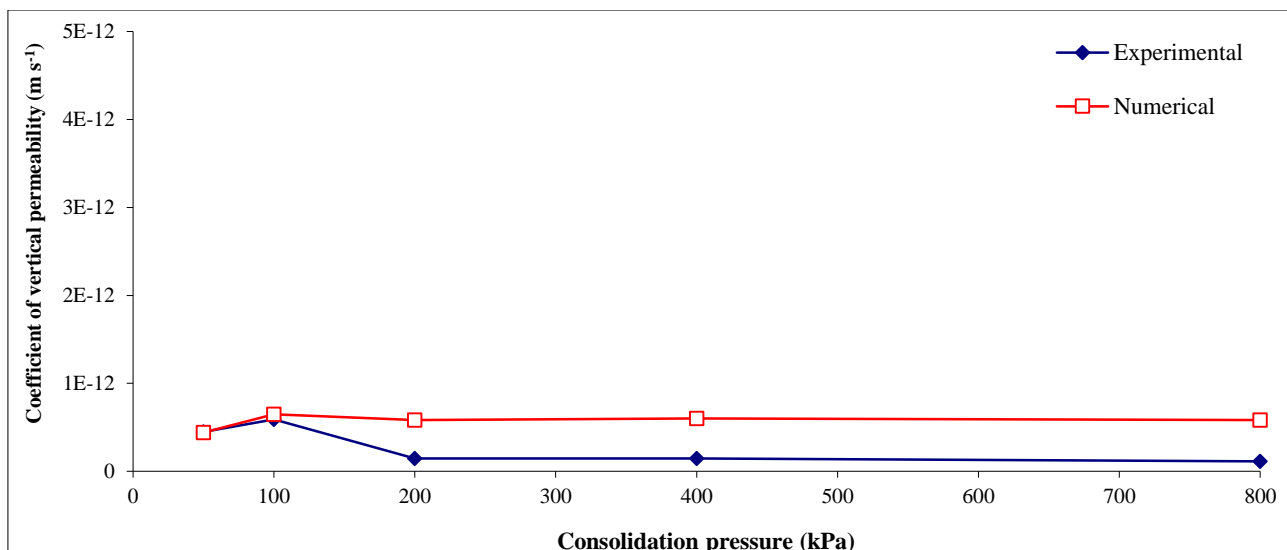


Figure 10. Trend of coefficients of vertical permeability of the stabilized peat over a range of consolidation pressures

8. Discussion

Although there was some drift in the final compression of the stabilized soil evaluated numerically in comparison to that evaluated experimentally in Figure 3, the difference between the two results was extremely small. This affirmed that compression of the stabilized soil was relatively small due to the slow rate of compression under various applied loadings as evident in both experimental and numerical results of c_v in Figure 7. Close agreement between experimental and numerical values of C_c and m_v of the stabilized soil as shown in Figures 8 and 9 respectively confirmed that the small compression of the stabilized soil was a direct result of small reduction in its void ratio. The small reduction in the void ratio of the stabilized soil can be linked to the soil hardening process as a result of its cement hydrolysis and pozzolanic activity. In a similar way, a reasonably good agreement between the results of laboratory test and numerical simulation of vertical displacement of foundation plate loaded on soil could be traced from the study of Krejci et al. [37].

Due to the brittle nature of the stabilized soil, it actually behaved like an elastic-plastic material. This is evident when the stabilized soil was subjected to the first consolidation pressure of 50 kPa for 7 days as shown in Figure 4, elastic compression predominated when it comprised of 75.6 % of the total compression of the stabilized soil. This provides an indication that the stabilized soil has large elastic strain which is a typical characteristic of hard soil. According to Whitlow [38], hard soils are likely to exhibit brittle failure by shearing.

The small and slow compression of the stabilized peat also implied that excess pore water pressure dissipation in the stabilized soil occurred at a very slow rate and thus, it exhibited extremely low permeability as verified by both of the experimental and numerical analyses on its k_v under the application of various consolidation pressures in Figure 10. In other words, a longer time is required under the application of each loading for the excess pore water pressure to dissipate from the stabilized soil. It must be noted that when pore pressure is extracted from saturated soil, pore water pressure will decline, which leads to the increase in the effective stress and the compression of soil skeleton [27]. Due to the domination of elastic compression in the stabilized soil, dissipation of excess pore water pressure from it had insignificant impact on its compressibility. Validation from the finite element solution on the exact solution regarding the compressibility of the stabilized soil proved that the strong interparticle bonding in it as a result of cement hydration process actually caused the stabilized soil to have slow rate of compression due to a load application. By comparison, it is also evident from the published work of Liu and Lei [3] that there was a close agreement in the results of pore water pressure isochrones for a one-layered soil calculated using the numerical and analytical inversion of Laplace transform. Liu and Lei [3] studied one-dimensional consolidation of layered soils with exponentially time-growing drainage boundaries.

9. Conclusions

In conclusion, comparison between the analytical and numerical solutions on the one-dimensional consolidation problem of stabilized peat indicated that there was a reasonable agreement between the two solutions. Results from the finite element analysis satisfactorily validated the experimental results based on analytical solution of the one-dimensional consolidation problem of the stabilized soil on the following remarks.

- The compression of the stabilized soil was very small due to its stiff and brittle behavior as a result of strong interparticle cementation bonds in it.

- The low values of c_v of the stabilized soil proved that its rates of compression under various application of loadings were slow due to the slow dissipation of excess pore water pressure from it.
- Values of C_c , m_v and k_v of the stabilized soil were relatively low due to its small reduction of void ratio under the application of loadings and the low ability of excess pore water to drain off from it.

10. Acknowledgements

The authors would like to express their deep appreciation to Universiti Tenaga Nasional (UNITEN) for providing necessary support to the research work of this paper. The authors would also like to acknowledge the funding contribution from the Ministry of Education (MOE) of Malaysia through Fundamental Research Grant Scheme (FRGS).

11. Funding

The research work for this paper was funded under Fundamental Research Grant Scheme (FRGS) (Project grant number: 20140107FRGS).

12. Conflict of Interest

The authors declare no conflict of interest.

13. References

- [1] Darrag A.A., El Tawil M.A., "The consolidation of soils under stochastic initial excess pore pressure", *Applied Mathematical Modelling*, 1993; 17, 609-612. doi:10.1016/0307-904X(93)90069-S.
- [2] Hebib S., Farrell E.R., "Some experiences on the stabilization of Irish peats", *Canadian Geotechnical Journal*, 2003; 40, 107-120. doi:10.1139/t02-09.
- [3] Liu J.C., Lei G.H., "One-dimensional consolidation of layered soils with exponentially time-growing drainage boundaries", *Computers and Geotechnics*, 2013; 54, 202-209. doi:10.1016/j.compgeo.2013.07.009.
- [4] Parron Vera M.A., Yakhlef F., Rubio Cintas M.D., Lopez C., Dubujet P., Khamlichi A., Bezzazi M., "Analytical solution of coupled soil erosion and consolidation equations by asymptotic expansion approach", *Applied Mathematical Modelling*, 2014; 38, 4086-4098. doi:10.1016/j.apm.2014.02.006.
- [5] Pauzi N.I.M., Omar H., Misran H., Othman S.Z., Manap A., "Settlement prediction of soil at closed dumping area using power creep function", *Applied Mechanics and Materials*, 2015; 773-774, 1542-1548. doi:10.4028/www.scientific.net/AMM.773-774.1542.
- [6] Xie K.H., Wang K., Chen G.H., Hu A.F., "One-dimensional consolidation of over-consolidated soil under time-dependent loading", *Frontiers of Architecture and Civil Engineering in China*, 2008; 2, 67-72. doi:10.1007/s11709-008-0009-7.
- [7] Xie K.H., Wang K., Wang Y.L., Li C.X., "Analytical solution for one-dimensional consolidation of clayey soils with a threshold gradient", *Computers and Geotechnics*, 2010; 37, 487-493. doi:10.1016/j.compgeo.2010.02.001.
- [8] Xie K.H., Li C.X., Liu X.W., Wang Y.L., "Analysis of one-dimensional consolidation of soft soils with non-Darcian flow caused by non-Newtonian fluid", *Journal of Rock Mechanics and Geotechnical Engineering*, 2012; 4, 250-257. doi:10.3724/SP.J.1235.2012.00250.
- [9] Xie K.H., Xia C.Q., An R., Hu A.F., Zhang W.P., "A study of the one-dimensional consolidation of double-layered structured soils", *Computers and Geotechnics*, 2016; 73, 189-198. doi:10.1016/j.compgeo.2015.12.007.
- [10] Zhuang Y.C., Xie K.H., "Study on one-dimensional consolidation of soil under cyclic loading and with varied compressibility", *Journal of Zhejiang University – Science*, 2005; 6A, 141-147. doi:10.1631/jzus.2005.A0141.
- [11] Du Y.J., Horpibulsuk S., Wei M.L., Suksiripattanapong C., Liu M.D., "Modeling compression behavior of cement-treated zinc-contaminated clayey soils", *Soils and Foundations*, 2014; 54, 1018-1026. doi:10.1016/j.sandf.2014.09.007.
- [12] Chao N.C., Lee J.W., Lo W.C., "Gravity effect on consolidation in poroelastic soils under saturated and unsaturated conditions", *Journal of Hydrology*, 2018; 566, 99-108. doi:10.1016/j.jhydrol.2018.08.081.
- [13] Moradi M., Keshavarz A., Fazeli A., "One dimensional consolidation of multi-layered unsaturated soil under partially permeable boundary conditions and time-dependent loading", *Computers and Geotechnics*, 2019; 107, 45-54. doi:10.1016/j.compgeo.2018.11.020.
- [14] Khabazian M., Mirghasemi A.A., Bayesteh H., "Compressibility of montmorillonite/kaolinite mixtures in consolidation testing using discrete element method", *Computers and Geotechnics*, 2018; 104, 271-280. doi:10.1016/j.compgeo.2018.09.005.
- [15] Yuan S., Zhong, H., "Consolidation analysis of non-homogeneous soil by the weak form quadrature element method", *Computers and Geotechnics*, 2014; 62, 1-10. doi:10.1016/j.compgeo.2014.06.012.

- [16] Zhang L., Ma M., Yang C., Wen Z., Dong S., "An investigation of pore water pressure and consolidation phenomenon in the unfrozen zone during soil freezing", *Cold Regions Science and Technology*, 2016; 130, 21-32. doi:10.1016/j.coldregions.2016.07.007.
- [17] Wong L.S., "Formulation of an optimal mix design of stabilized peat columns with fly ash as a pozzolan", *Arabian Journal for Science and Engineering*, 2015; 40, 1015-1025. doi:10.1007/s13369-015-1576-2.
- [18] Baral P., Rujikiatkamjorn C., Indraratna B., Kelly R., "Radial consolidation characteristics of soft undisturbed clay based on large specimens", *Journal of Rock Mechanics and Geotechnical Engineering*, 2018; 10, 1037-1045. doi:10.1016/j.jrmge.2018.06.002.
- [19] Wang L., Xu Y., Xia X., Sun D., "Semi-analytical solutions to two-dimensional plane strain consolidation for unsaturated soil", *Computers and Geotechnics*, 2018; 101, 100-113. doi:10.1016/j.compgeo.2018.04.015.
- [20] Terzaghi, K. *Erdbaumechanik auf bodenphysikalischer Grundlage*, Leipzig und Wien, F. Deuticke, 1925.
- [21] Terzaghi, K. *Theoretical soil mechanics*, John Wiley & Sons, New York, 1943. doi:10.1002/9780470172766.
- [22] Terzaghi, K., Peck, R.B. *Soil mechanics in engineering practice*, John Wiley & Sons, New York, 1948.
- [23] Liu Q., Deng Y.B., Wang T.Y., "One-dimensional nonlinear consolidation theory for soft ground considering secondary consolidation and the thermal effect", *Computers and Geotechnics*, 2018; 104, 22-28. doi:10.1016/j.compgeo.2018.08.007.
- [24] Ho L., Fatahi B., "Analytical solution for the two-dimensional plain strain consolidation of an unsaturated soil stratum subjected to time-dependent loading", *Computers and Geotechnics*, 2015; 67, 1-16. doi:10.1016/j.compgeo.2015.02.011.
- [25] Bardet J.P. *Experimental soil mechanics*, Prentice-Hall, New Jersey, 1997.
- [26] Meidani M., Chang C.S., Deng Y., "On active and inactive voids and a compression model for granular soils", *Engineering Geology*, 2017; 222, 156-167. doi:10.1016/j.enggeo.2017.03.006.
- [27] Li Z., Cui Z.D., "Axisymmetric consolidation of saturated multi-layered soils with anisotropic permeability due to well pumping", *Computers and Geotechnics*, 2017; 92, 229-239. doi:10.1016/j.compgeo.2017.08.015.
- [28] Kreyszig E. *Advanced engineering mathematics*, tenth ed., John Wiley & Sons, Singapore, 2011. doi:10.1002/bimj.19650070232.
- [29] Head K.H. *Manual of soil laboratory testing*, third ed., Whittles Publishing, London, 2006.
- [30] Tagar A.A., Changying J., Adamowski J., Malard J., Shi Qi C., Qishuo D., Abbasi N.A., "Finite element simulation of soil failure patterns under soil bin and field testing conditions", *Soil & Tillage Research*, 2015; 145, 157-170. doi:10.1016/j.still.2014.09.006.
- [31] Rao, S.S. *The finite element method in engineering*, fifth ed., Butterworth-Heinemann, London, 2005. doi:10.1016/B978-0-7506-7828-5.X5000-8.
- [32] Logan D.L. *A first course in the finite element method*, sixth ed., Thomson, Toronto, 2016.
- [33] Brinkgreve R.B.J. *PLAXIS 2D-Version 8*, first ed., A.A. Balkema, Delft, 2002.
- [34] Dhatt G. and Touzot G. *The finite element method displayed*, John Wiley & Sons, Norwich, 1984. doi:10.1002/zamm.19850650729.
- [35] Wong L.S., Hashim R., Ali F., "Engineering behaviour of stabilized peat soil", *European Journal of Scientific Research*, 2008; 21, 581-591.
- [36] Silva R.P., Rolim M.M., Gomes I.F., Pedrosa E.M.R., Tavares U.E., Santos A.N., "Numerical modeling of soil compaction in a sugarcane crop using the finite element method", *Soil & Tillage Research*, 2018; 181, 1-10. doi:10.1016/j.still.2018.03.019.
- [37] Krejci T., Koudelka T., Broucek M., "Numerical modelling of consolidation processes under the water level elevation changes", *Advances in Engineering Software*, 2014; 72, 166-178. doi:10.1016/j.advengsoft.2013.08.005.
- [38] Whitlow R. *Basic soil mechanics*, fourth ed., Pearson Education, London, 2001.

I. Appendix

According to Brinkgreve [22], the equilibrium and continuity equations considered in the finite element computation of PLAXIS 2D 8.2 Professional version software on the consolidation problem can be expressed in a block matrix equation as in Equation A.1.

$$\begin{bmatrix} K & L \\ L^T & -S \end{bmatrix} \begin{bmatrix} \frac{dv}{dt} \\ \frac{dp_n}{dt} \end{bmatrix} = \begin{bmatrix} 0 & 0 \\ 0 & H \end{bmatrix} \begin{bmatrix} v \\ p_n \end{bmatrix} + \begin{bmatrix} \frac{df_n}{dt} \\ q_n \end{bmatrix} \quad (\text{A.1})$$

By employing a simple step by step integration procedure, the equation is solved iteratively. Assigning the symbol Δ to represent finite increments, the integration yields Equation A.2.

$$\begin{bmatrix} K & L \\ L^T & -S^* \end{bmatrix} \begin{bmatrix} \Delta v \\ \Delta p_n \end{bmatrix} = \begin{bmatrix} 0 & 0 \\ 0 & \Delta t H \end{bmatrix} \begin{bmatrix} v_0 \\ p_{n0} \end{bmatrix} + \begin{bmatrix} \Delta f_n \\ \Delta t q_n^* \end{bmatrix} \quad (\text{A.2})$$

Where

$$S^* = \alpha \Delta t H + S$$

$$q_n^* = q_{n0} + \alpha \Delta q_n$$

α = Time integration coefficient

K = Stiffness matrix

L = Coupling matrix

v = Nodal displacement vector

p_n = Excess pore water pressure vector

t = Surface tractions

f_n = Load vector

$$H = (\nabla N)^T R \nabla N / \gamma_w dV$$

N = Interpolation functions

R = Permeability matrix

γ_w = Unit weight of water

dV = Integration over the volume of the body considered